No evidence from MVPA for different processes underlying the N300 and N400 incongruity effects in object-scene processing.

Dejan Draschkow[1], Edvard Heikel[1], Melissa L.-H. Võ[1], Christian J. Fiebach[1,2], & Jona Sassenhagen[1]

[1] Department of Psychology, Goethe University Frankfurt, Theodor-W.-Adorno-Platz 6, Frankfurt am Main 60323, Germany

[2] Brain Imaging Center, Goethe University Frankfurt, Frankfurt am Main, Germany

Corresponding author contact information:

Dr. Dejan Draschkow
Scene Grammar Lab
Department of Cognitive Psychology
Goethe University Frankfurt
PEG, Room 5.G105
Theodor-W.-Adorno-Platz 6
60323 Frankfurt am Main, Germany

Phone: +49 (0)69 798 35310
Mail: draschkow@psych.uni-frankfurt.de
Web: www.draschkow.com; www.SceneGrammarLab.com

Keywords: *Scene processing; Object recognition; Scene grammar; EEG; N400; N300*

Acknowledgments**:** This work was supported by DFG grant VO 1683/2-1 and by SFB/TRR 135 project C7 to MLV and by an ERC Consolidator grant (agreement no. 617891) awarded to CJF. We wish to thank Aylin Kallmayer, Maximilian Scheuplein and Daniela Gresch for valuable help with data collection. We thank Sage Boettcher for comments and discussion. We also would like to thank the two anonymous reviewers for their extremely constructive suggestions and comments.

Abstract

Attributing meaning to diverse visual input is a core feature of human cognition. Violating environmental expectations (e.g., a toothbrush in the fridge) induces a late event-related negativity of the Event-Related Potential/ERP. This *N400* ERP has not only been linked to the semantic processing of language, but also to objects and scenes. Inconsistent object-scene relationships are additionally associated with an earlier negative deflection of the EEG signal between 250-350 ms. This *N300* is hypothesized to reflect pre-semantic perceptual processes. To investigate whether these two components are truly separable or if the early object-scene integration activity (250-350 ms) shares certain levels of processing with the late neural correlates of meaning processing (350-500 ms), we used time-resolved multivariate pattern analysis (MVPA) where a classifier trained at one time point in a trial (e.g., during the N300 time window) is tested at every other time point (i.e., including the N400 time window). Forty participants were presented with semantic inconsistencies, in which an object was inconsistent with a scene's meaning. Replicating previous findings, our manipulation produced significant N300 and N400 deflections. MVPA revealed above chance decoding performance for classifiers trained during time points of the N300 component and tested during later time points of the N400, and vice versa. This provides no evidence for the activation of two separable neurocognitive processes following the violation of context-dependent predictions in visual scene perception. Our data supports the early appearance of high-level, context-sensitive processes in visual processing.

1. Introduction

Learned regularities and previous experience with our visual environment regulate predictions about *which* objects should occur *where* in a scene, alleviating the computational load of perceptual processes (Bar, 2004, 2007, 2009; Biederman, 1981; Biederman, Mezzanotte, & Rabinowitz, 1982). For example, objects that are not easily identifiable when presented without scene context can be easily identified if the scene background is provided (Brandman & Peelen, 2017). These predictions can be investigated by showing observers images containing violations of different forms. Thus, seeing a bathtub in a living room would violate what we have interpreted in previous work as *semantic* predictions about what object belongs in the scene, while finding a toilet brush next to the toothpaste would violate *spatial* predictions (Draschkow & Võ, 2017; Võ & Wolfe, 2013, 2015). These paradigms have revealed that violations of predictions can lead to slower and less accurate identification of objects (Bar, 2004; Biederman et al., 1982; Davenport & Potter, 2004), elicit longer and more frequent fixations on critical objects (Cornelissen & Võ, 2016; Henderson, Weeks, & Hollingworth, 1999; Loftus & Mackworth, 1978), and impede visual search (Castelhano & Heaven, 2011; Võ & Henderson, 2010). Studies of brain correlates of meaning in language identified a late event-related negativity (N400) sensitive to violations of semantic expectations (Kutas & Federmeier, 2011; Kutas & Hillyard, 1980). Object-scene violations are accompanied by a similar, yet more anteriorly distributed negativity: a scene N400 (Ganis & Kutas, 2003; Kovalenko, Chaumon, & Busch, 2012; McPherson & Holcomb, 1999; Mudrik, Lamy, & Deouell, 2010; Võ & Wolfe, 2013). It is hypothesized to accompany semantic processing of scenes.

Inconsistent object-scene relationships are additionally associated with an earlier negative component (250-350 ms) – often referred to as N300. McPherson and Holcombe (1999) first demonstrated that objects preceded by an unrelated prime elicit a more frontally

distributed event-related negativity around 300ms, supporting the existence of two separate components, an anterior, image-specific N300 and a later, central/parietal concept-level N400. Ever since this initial finding, many studies using visual objects and scenes have used this terminology and/or have separated their analysis according to these proposed components (e.g., Federmeier & Kutas, 2001; Hamm, Johnson, & Kirk, 2002; Meade, Lee, Midgley, Holcomb, & Emmorey, 2018; Mudrik et al., 2010; Mudrik, Shalgi, Lamy, & Deouell, 2014; Sitnikova, Holcomb, Kiyonaga, & Kuperberg, 2008; Võ & Wolfe, 2013; Willems, Özyürek, & Hagoort, 2008). The N300 is hypothesized to reflect pre-semantic perceptual processes (Mudrik et al., 2010; Schendan & Kutas, 2002; Schendan & Maher, 2009) and in a direct comparison, Hamm et al. (2002) argued that the N300 and N400 are generated by distinct underlying networks of cortical activity and reflect two distinct semantic effects in object identification – categorization and amodal semantic mismatches respectively.

There is, however, also a body of evidence suggesting that the separation of these components might be artificially imposed due to data preprocessing, task (e.g. quicker access to pictures compared to words due to a less arbitrary relationship between object/scene pairs) and/or participant specific variance in the temporal manifestation of a single component. Thus, it cannot be fully excluded on the basis of the available empirical literature that the topographic differences might only be superficial in nature. This notion receives support from several lines of evidence: Willems et al. (2008) failed to observe a separate N300 effect and accordingly argued against this component being specific to the processing of pictures. Previous studies have also either failed to find a distinguishable N300 effect (Demiral, Malcolm, & Henderson, 2012; Federmeier & Kutas, 2001; Ganis & Kutas, 2003; Nigam, Hoffman, & Simons, 1992), or found a similar time-course between the N400 of words and pictures, but diverging topographies (Ganis, Kutas, & Sereno, 1996). Further, it is possible that even with superficial differences in topography, the exact same neural structures are engaged during these time windows and an overlap of a late posterior positivity from the P3

family results in the apparent reduction of the N400 effect at parietal and posterior scalp sites (Nobre & McCarthy, 1994). Finally, it can be questioned whether the early scene-specific N300 effect is at all exclusive for pictorial stimuli, as its time window (i.e., starting around 250 ms and ending at 350 ms) overlaps with the well-established time course of the N400 often reported in language studies (250-500 ms; e.g. Kutas & Federmeier, 2011).

The potential separability of N300 and N400 may ultimately not be resolvable using classical ERP analyses, as their ability to identify differences in the underlying neural substrate of two ERP components with similar scalp distributions is inherently limited. As shown by Kutas and Urbach (2002), common statistical procedures intended to identify a dissimilarity of the underlying source configuration do not in fact do so. A promising novel tool for identifying dissimilarities vs. commonalities of EEG signals across time is time-generalized multivariate decoding (e.g., King & Dehaene, 2013), which has also been applied to investigating the N400 component in language (Heikel, Sassenhagen, & Fiebach, 2018). Time-generalized decoding consists of training machine learning classifiers to distinguish between experimental conditions at each point throughout the trial, based on their specific patterns of EEG activity. The resulting fitted classifiers are then each evaluated at all time-points. Applying this method to the investigation of N300 vs. N400 responses to object-scene inconsistency, one can train classifiers to learn neural patterns separating congruent from incongruent conditions during the N300 time window, and then test how well these classifiers perform when applied to classify N400 time window activity (and vice versa). While still operating in the space of scalp-recorded topographical patterns (and not, e.g., in source space representing the generators of the underlying neural processes), this procedure allows one to positively quantify the degree of overlap and similarity between neural patterns at different time points. This bottom-up, data-driven approach, accordingly, transcends a theory-

126 motivated, or descriptive, segmentation of the event-related potential into arbitrary windows,
127 providing a more objective look at sequences of processing stages.

128 In our specific case, we leverage time-generalized decoding to test whether or not the
129 congruence effect during the N300 window differs from that during the N400 window. While
130 not being conclusive proof for identity vs. non-identity, given the inherent limitations of scalp
131 EEG and the nature of falsificationist hypothesis testing, the possible results clearly map onto
132 different hypotheses. If N300 and N400 effects reflect just one continuous process, classifiers
133 trained during the N400 time window should perform well during the N300 time window, and
134 vice versa. If, however, the two ERP effects reflect different cognitive stages in a processing
135 chain with different cortical substrates, then no generalization should be found between N300
136 and N400. Note that the results of this analysis can speak only to a *neurocognitive* theory of
137 differences in the underlying neurocognitive events. It is, in principle, possible that N300 and
138 N400 window reflect one and the same cortical source configuration (in which case
139 substantial temporal generalization should be observed), but very different cognitive
140 computations (performed by one and the same brain area). However, finding such N300/N400
141 cross-decoding would argue against strong interpretations of N300 and N400 time windows
142 as reflecting two different cognitive processing stages.

2. Methods

2.1. Participants

Participants were recruited at the Goethe University Frankfurt, until forty complete data sets were obtained (mean age = 21.8, range = 18-41, 33 female, 4 left-handed). As this is the first analysis of its kind, no sensible power analysis could be conducted; we instead simply chose a sample size that is large compared to similar studies (Mudrik et al., 2010; Võ & Wolfe, 2013), while still being feasible. All participants had normal or corrected-to-normal vision. All were volunteers receiving course credit or financial compensation and had given informed consent according to protocols approved by the local ethics committee. None reported a history of neurological or psychiatric disorders.

2.2. Stimuli and procedure

The stimulus material (318 saliency controlled images of real-world scenes) and procedure were nearly identical to the study of Võ and Wolfe (2013). The 318 images consisted of 152 unique scenes in either a semanitcally consistent or inconsistent version (i.e., the object was either from the same category as the scene or not), as well as 10 additional scenes used as targets for a repetition detection task and 4 practice images. Stimuli were presented in a dimly-lit room using OpenSesame (Mathôt, Schreij, & Theeuwes, 2012) on a 24-inch monitor (resolution = 1920 × 1080, viewing distance approx. 65cm, scenes subtending approx. 24° (horizontal) by 18° (vertical) of visual angle).

Participants were told that they would see a series of scenes, each containing one critical object marked by a cue. Each trial began with a blink phase. The participant could initiate the trial by pressing the spacebar, which was followed by the presentation of a scene without the critical object for 500ms. Next, a red dot appeared at a location in the scene, indicating where to move the eyes and where to expect the critical object to appear. Five hundred milliseconds after onset of the cue (plus a random jitter between 0 and 300ms, to prevent anticipatory

effects), the critical object appeared in the scene and remained visible together with the scene for 2,000ms (Figure 1). To keep participants engaged in viewing the scenes without explicitly probing the object-scene inconsistencies, we asked them to view each scene carefully and to press a button whenever they spotted an exact repetition (i.e., the same scene with the same object in the same location as seen on a previous trial).

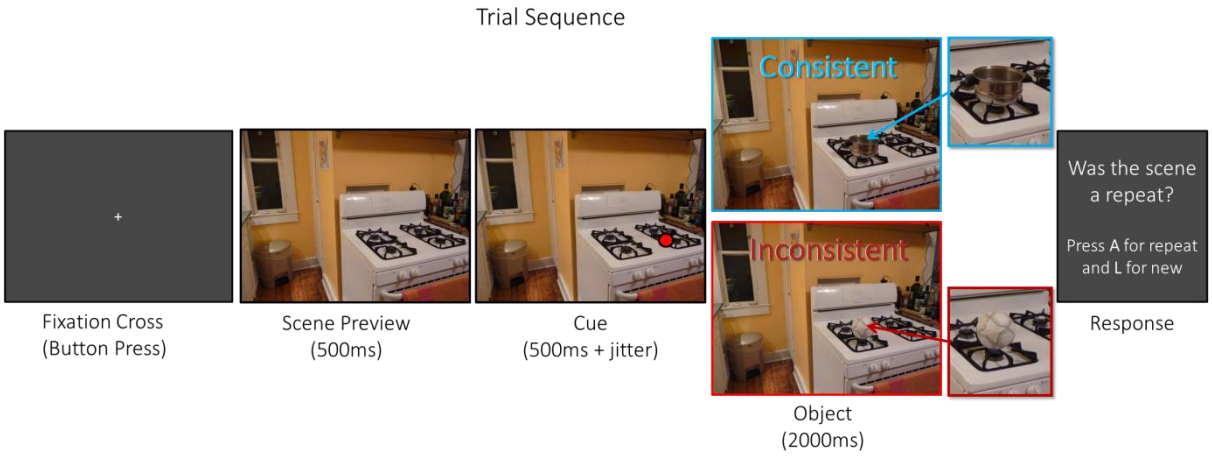

Figure 1: Trial sequence. Each trial started with the presentation of a fixation cross that indicated blinking was encouraged. Once ready, subjects pressed a button, which triggered the presentation of a preview scene without the critical object (500 ms). Next, a cue appeared (500 ms plus randomly sampled jitter between 0-300 ms), and participants moved their eyes to the cued location. Then the object appeared at the cued location and remained visible on the screen together with the scene (2,000 ms). The object could either be consistent or inconsistent with the scene. Finally, the participants indicated if they had seen the current object-scene combination before during the experiment.

The 169 experimental trials included 152 unique and 17 repetition trials. Each of the 152 unique scenes was used in either a semantically consistent or inconsistent version (Figure 1), resulting in 76 trials per condition. Each participant saw each of the scenes only once during the event-related potential (ERP) experiment, except for the additional 17 trials containing repeated (i.e. target) scenes for a repetition detection task. All target scenes for the repetition detection task were excluded from subsequent analysis (i.e., their first and subsequent presentations), thus the analysis was conducted on data from the 152 experimental trials. Assignment of scenes to the two conditions was counterbalanced across participants and the order of scene presentation was random. Participants were acquainted with the procedure

through 4 practice trials before the start of the experiment. The experiment lasted ~30 minutes.

2.3. Data acquisition and pre-processing

The complete pre-processing and analysis scripts can be found alongside the experimental data as html files and as reproducible scripts (jupyter notebooks; (Kluyver et al., 2016)) at https://github.com/DejanDraschkow/n3n4).

The electroencephalogram (EEG) was recorded with a sampling rate of 1,000Hz from 64 active Ag/AgCl electrodes (arranged in an extended 10-20 layout using either a brainAmp amplifier or an actiChamp amplifier (both: Brain Products GmbH, Gilching, Germany). EEG data analysis was conducted in MNE-Python (Gramfort et al., 2013; https://mne-tools.github.io/). First, data was referenced to linked mastoid electrodes. Then, it was down-sampled to 200Hz, high-pass filtered at 0.1Hz and low-pass filtered at 40Hz. Eye movements and muscle artefacts were corrected via independent component analysis (ICA; Jung et al., 2000). ICA components were estimated on data which was high-pass filtered at 8Hz using FastICA. Eye movement components were detected by (1) correlating the filtered data with the electrooculography (EOG) signal plus (2) manually selecting a subset of typical component maps and identifying the best group match to them (Viola et al., 2009). Selected components were then removed from the 0.1Hz filtered data and a 20Hz low-pass filter was applied.[1] Then, EOG channels were dropped, leaving 60 channels in total. Subsequently, data was segmented into 1100-ms epochs time-locked to the onset of the cued object (i.e., -200 to +900 ms relative to target stimulus onset). Each epoch was baseline-adjusted by subtracting the mean amplitude in the prestimulus period (−200 ms to 0 ms) from all the data points in the epoch. Finally, fully automated artifact rejection with default values using peak-to-peak

[1] We also repeated the MVPA analyses on data filtered even more modestly – below 55 Hz – to exclude artificially induced temporal generalization. Due to the much lower signal to noise ratio, overall decoding accuracies were lower; nevertheless, the qualitative pattern of results did not change.

thresholding was used to interpolate artefactual channels and to drop contaminated epochs (Jas, Engemann, Bekhti, Raimondo, & Gramfort, 2017), leaving on average 149 trials (132-152) per subject, with a mean of 74.6 trials in the consistent and 74.4 in the inconsistent condition.

2.4. Data analysis

Univariate analysis: Event-related brain potentials (ERPs) were calculated by first averaging trials within subjects, and then averaging these waveforms across subjects, separately for consistent and inconsistent trials. For statistical analysis, the mean amplitudes were calculated for two consecutive time windows, i.e., 250-350ms (N300) and 350-500 (N400), across the mid-central region (electrodes FC1, FCz, FC2, C1, Cz, C2, CP1, CPz, and CP2) which was previously shown to display strong scene-related N300 and N400 effects (Ganis & Kutas, 2003; Mudrik et al., 2014; Võ & Wolfe, 2013). Paired sample *t*-tests were used for the critical comparisons between conditions.

Multivariate pattern analysis: To test to which degree similar neural patterns occur at different time points of object-scene integration, a multivariate pattern analysis (MVPA) was implemented on the epoched EEG data. Independently for each subject, a Logistic Regression implemented in scikit-learn (Pedregosa et al., 2011), with default parameters, was trained to classify trials as being consistent or inconsistent based on brain activity. Classifiers were trained separately on EEG activity at each time point. A 5-fold stratified cross-validation procedure with balanced classes (i.e., equal number of consistent vs. inconsistent trials per fold, within each subject) was used: Each participant's epochs were split into five equal-sized folds. For each time point in each epoch in a fold, trial type (inconsistent vs. consistent) was predicted by a classifier that had been fitted (i.e., 'trained') on the other four folds. To assess the quality of the predictions - i.e., correctly vs. incorrectly labelled trials – the Area under the Curve of the Receiver-Operating Characteristic was calculated, as a sensitive, yet robust

scoring procedure: higher scores (on a scale from 0 to 1) indicate that brain activity more strongly differs between the two conditions (with .5 corresponding to guessing, and 1 to perfect accuracy).

To investigate if neurocognitive patterns are shared between early and late stages of the N300/N400 complex, MVPA was applied in a time-generalized manner (King & Dehaene, 2014). In this procedure, a classifier is not only tested at the time point it was trained on (e.g., during the N300 time window), but also used for predicting the condition of the trial at every other time point (i.e., including the N400 time window). This is schematically illustrated in Figure 2. Calculating classification scores based on EEG activity at each time for classifiers trained at each time point results in a Generalization Across Time/GAT matrix (Figure 5A) that shows training times on the y-axis against testing times on the x-axis. The diagonal of this GAT matrix represents training and testing at the same time point (e.g., trained at 350 ms and tested on 350 ms) – i.e., the strength of the neural pattern dissociating violation from control trials. Off-diagonal entries show pattern persistence or re-occurrence – that is, time points t+x where a classifier trained at time point t can still successfully classify trials, indicating that similar EEG patterns, and thus, by inference, similar cognitive processes, characterize both time points. If the N300 was functionally distinct from the N400, one would expect that classifiers trained during the N300 time windows would not generalize well to later time points of the N400 component. Demonstrating above chance classification accuracy of these classifiers (i.e., temporal generalization from N400 to N300, and the reverse) would however indicate that similar neural patterns are generating the two components.

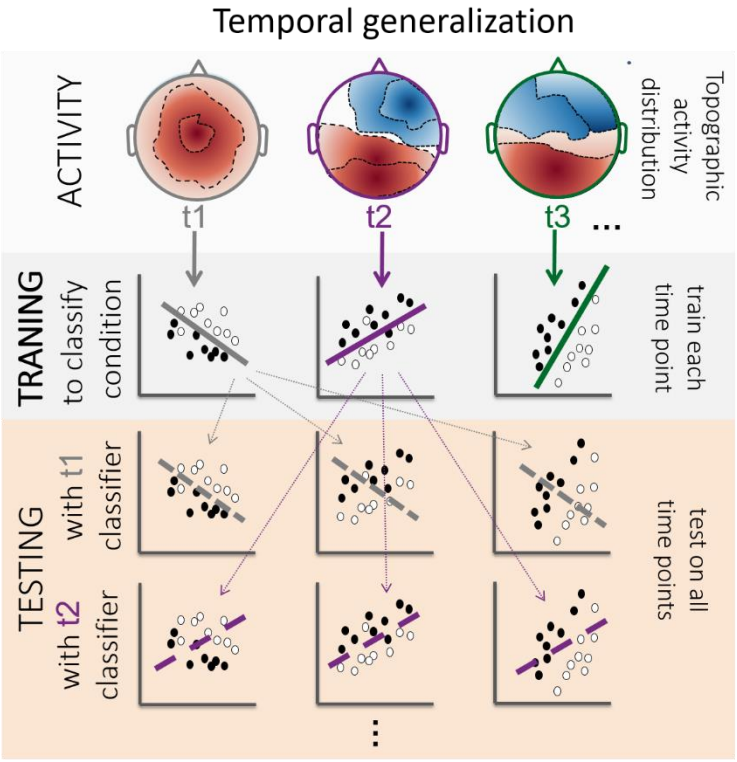

Figure 2: Visualization of the generalization across time (GAT) procedure. First row: at time points in the trial where neurocognitive processes differ between two experimental conditions, distinct spatio-temporal responses are evoked which appear on individual trials (mixed with noise). MVPA methods use powerful pattern classifications algorithms to learn multivariate patterns that distinguish between the condition-specific EEG responses (second row). To test whether neurophysiological patterns generalize to other time points, a classifier trained at one time point (t) is also scored concerning its predictions based on neurophysiological patterns at all other time points, i.e. testing at time point t2, t3, etc. This procedure is repeated for all time points of a trial.

Statistical analysis: Time-generalized decoding scores were statistically evaluated in the two time windows introduced above, i.e., N300 and N400, thereby tracking over the time course of the entire epoch the classification accuracy scores of classifiers trained on data from these two time windows. Specifically, the performance of N300 vs. N400 classifiers over time was evaluated by (1) separately averaging the accuracy scores of all classifiers that were trained on the data points from the two non-overlapping time windows (i.e., 250-350ms and 350-500ms, respectively), and then (2) inferential testing their classification accuracy against chance (.5) or against each other (N300 vs. N400). Diagonal decoding scores were analyzed in the same way. GAT matrices were subjected to the same procedure.

For time series and GAT matrices, statistical results were subjected to Threshold-Free Cluster Enhancement/TFCE (Smith & Nichols, 2009), implemented in MNE Python. TFCE is a nonparametric method for identifying statistically significant contrasts that derives statistical power from the cluster structures in the data (Maris & Oostenveld, 2007). It does not require selecting parameter values. TFCE controls for multiple comparisons, while retaining high sensitivity.

To investigate if classifiers trained in one time window outperformed those trained in the other time, mean scores of all decoders trained on one time window were averaged first within the training window, and then within the other window (i.e., N300 classifiers -> N300 time window, N300 classifiers -> N400 time window, etc.). If the N300 classifiers outperformed N400 classifiers during the N300 window, this would indicate that there were distinct patterns occurring only during the N300 time window, and which could therefore only be learned by N300-trained classifiers. To quantify if there was any effect specific to the N300 window that could not be explained by N400 window decoders, the 95% bootstrapped confidence interval for the difference between N300->N300 and N400->N300 cross-decoding was calculated, as well as for N400->N400 vs. N300->N400.

Finally, we conducted two analyses on aggregate activity in the N300 and N400 time windows[2]. First, we repeated the above analysis, but averaged across time points in a preceding step. Next, it might be argued that the method we employ here could only ever produce evidence in favor of two distinct patterns in the form of a negative finding: an inability to cross-decode. We implemented an analysis capable of providing positive evidence in the following form: separately for each dataset and each trial, we averaged activity in the N300 and the N400 time window. Then, we trained a classifier (Logistic Regression and 5-fold cross-validation; i.e.., as before) to predict, based on these values, if a pattern was extracted from the N300 or the N400 time window. To ensure that temporal autocorrelation

[2] We thank an anonymous reviewer for suggesting these two analyses.

did not bias the classifier, we split the trials in half, i.e., putting N300 time window activity for all even trials and N400 activity for all odd trials in one run, and the remaining trials in another, and averaged the results. A positive outcome would indicate that the classifier could pick up on neural patterns indicating if the trial was from the early or the late time window. We calculated via bootstrapping the 95% confidence interval across datasets for the resulting decoding scores.

3. Results

Behavioral analysis: The overall error rate on the repetition detection task averaged 5.5% (*SD*=3.7%). The false alarm rate, i.e., participants erroneously reporting a unique scene as a repeat, was 2.6% (*SD*=4.1%).

3.1. ERP results

Replicating previous findings, in the N300 time window (250–350 ms), semantic violations elicited a significantly more negative response than the consistent control condition, $t(39) = 4.52$, $p < .001$ (see Fig. 3A). The same was true for the N400 time window (350–500 ms), $t(39) = 5.14$, $p < .001$. Visualizing the spatiotemporal structure of contrast effects for N300 and N400 time windows (see Fig. 3B) indicated highly similar patterns.

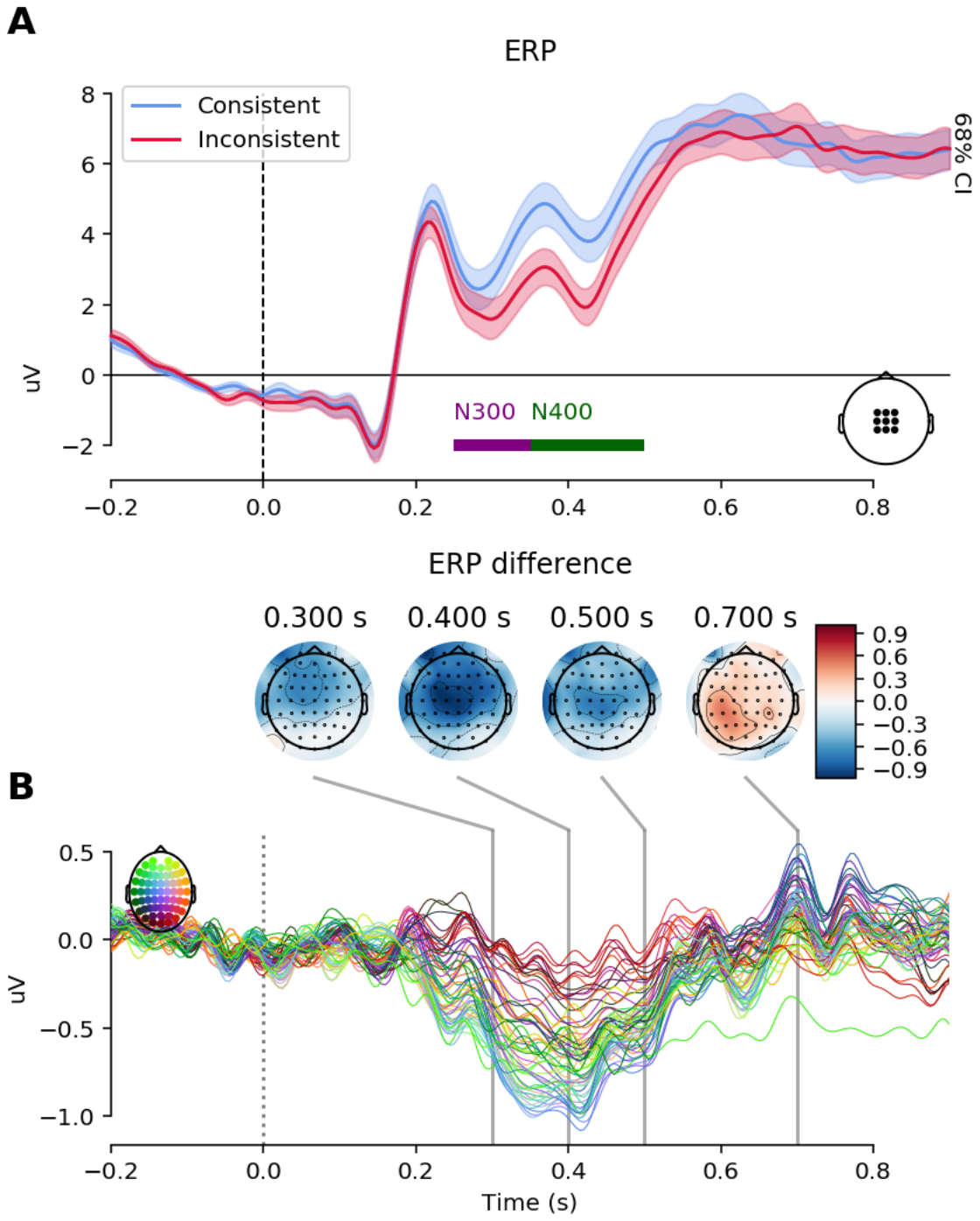

Figure 3: Event-related potentials, consistent vs. inconsistent. A: ERP time-locked to scene plus object onset, for consistent and inconsistent conditions, at central electrodes. Shaded region indicates a 68% confidence interval. Purple and dark green horizontal bars indicate N300 and N400 time windows. B: Joint Butterfly + topographical map plot of inconsistent minus consistent difference. Each colored line represents one channel; see colored inset legend (left) for locations on the EEG cap. Adjacent channels receive adjacent colors. Additionally, topographical maps are shown for representative time points. Topomaps indicate the similarity of patterns at 300, 400 and 500 ms; colored line plots show that these patterns are representative for the entire time course of the negative-polarity ERP effect.

3.2. MVPA results

In agreement with raw ERP results, examining the distribution of patterns across time reinforces the interpretation that essentially the same neural pattern is expressed throughout the 200-550 msec range. Note that all multivariate analyses are not based on channel pre-selection, instead taking into account the full topographic distribution.

Temporally resolved decoding indicated above-chance decoding beginning around 200 msec after stimulus onset (Fig. 4A), i.e., it was possible to classify trials as consistent vs. inconsistent based on brain activity. The corresponding classifier patterns (i.e., the neural patterns dissociating brain activity in inconsistent vs. consistent trials) are shown in Figure 4B. Much like scalp topographies of raw ERP differences, classifier patterns throughout the N300 and N400 windows (extracted by the method presented by Haufe et al., 2014) were visually highly similar both throughout the time windows, and compared to the ERP results.

Classifiers trained during any of these windows showed statistically significant above-chance decoding throughout the entire time window, as evidenced by the Generalization Across Time matrix displayed in Figure 5A; e.g., a classifier trained on EEG data at 400 msec after stimulus presentation (y-axis, 400 msec) could successfully classify trials based on EEG activity at 300, 400 and 500 msec (x-axis, 300, 400, 500 msec).

To quantify the separability of neural processes reflected in the N300 vs. N400 time windows, we averaged the time-courses of performance scores of all classifiers trained between 250 and 350 ms (‘*N300 classifier’*) and of all classifiers trained between 350 and 500 ms (‘*N400 classifier’*). Figures 5B and C show the degree to which N300 and N400 classifiers can decode trial type at different time points in the trial. The temporal evolution of the decoding performance of both classifiers across the entire trial epoch is shown in Figure 5B. Both classifiers demonstrated significant decoding performance throughout the entire duration of the N300/N400 complex, starting as early as ~200 ms post object onset (p<0.05).

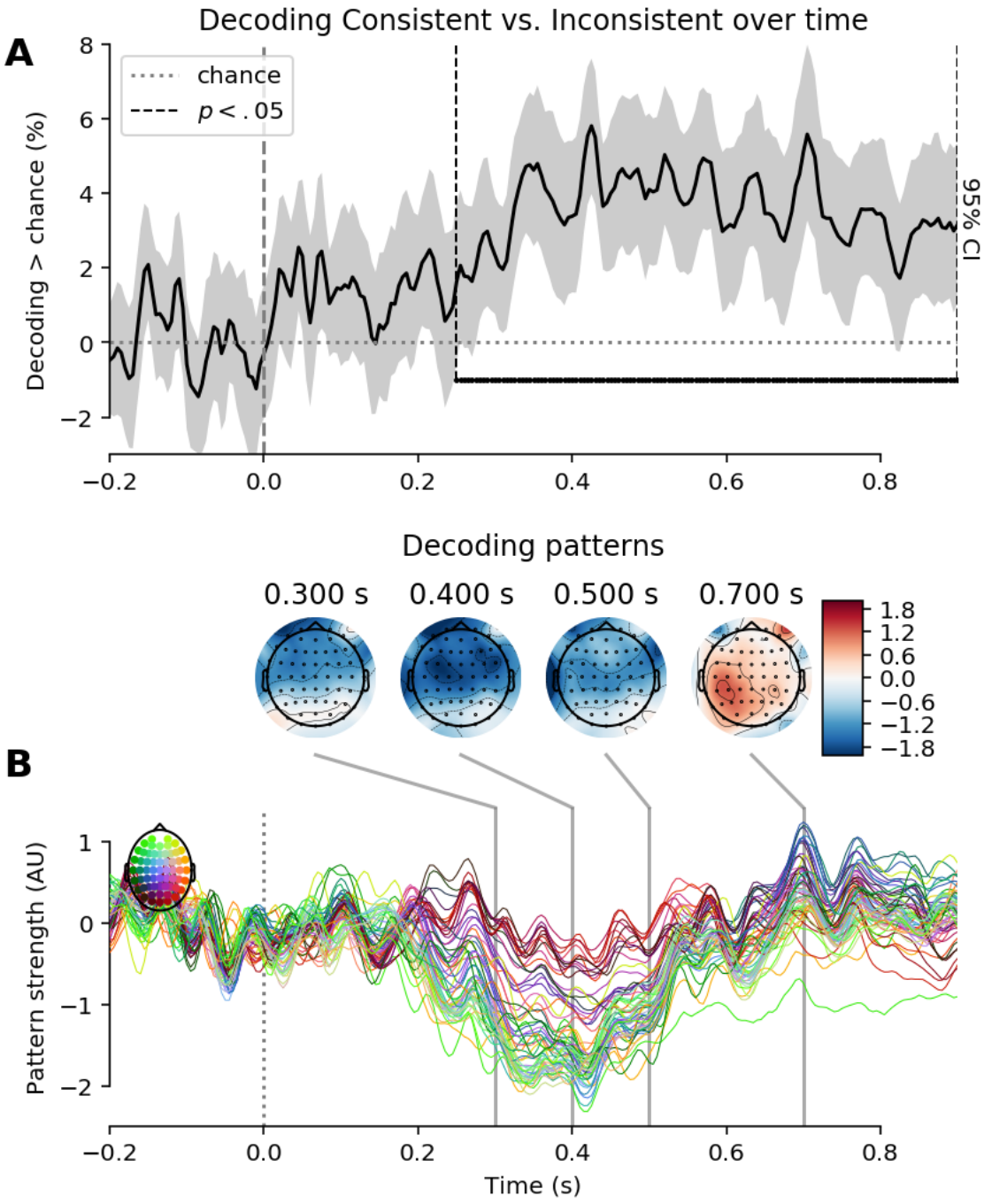

357

358 **Figure 4: Decoding across time. A: Temporally resolved decoding of inconsistent vs. consistent trials, for each time point.**
359 **Thick horizontal black line indicates statistically significant (p < .05, TFCE) time points. Shaded region indicates 95%**
360 **confidence interval. B: corresponding spatial patterns learned by the decoder, separately at each time point, visualized**
361 **as the ERP contrast in 3B (joint Butterfly + topographical map plot). Patterns were extracted from decoder coefficients**
362 **via the technique discussed by Haufe et al. (2014).**

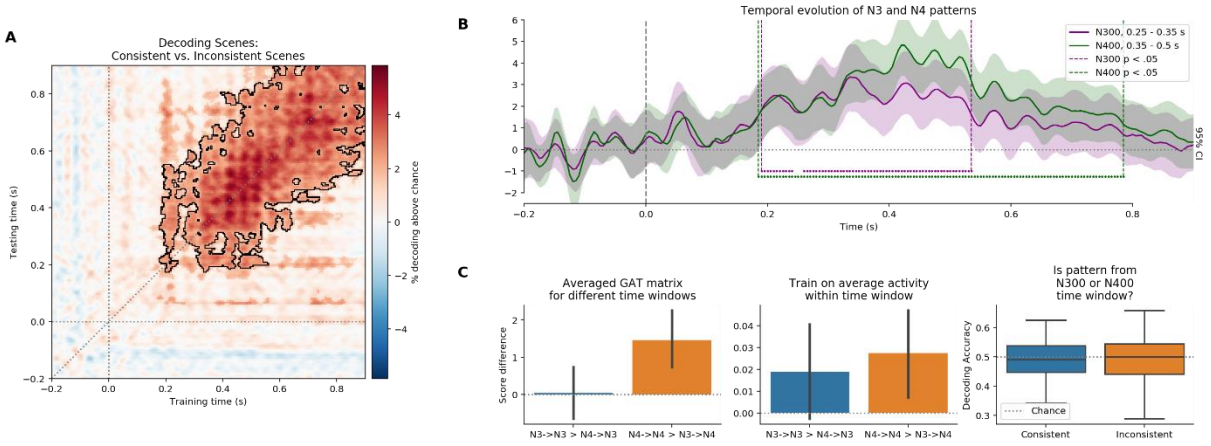

Figure 5: Time-resolved decoding. A: GAT matrix. Decoding accuracy above chance (warmer colors indicate better performance) is plotted as a function of time points used for training the classifier (Y-axis) and time points used to test the classifier (X-axis). Diagonal corresponds to 4A. Areas not significant at $p < .05$ (TFCE) are set to transparent; areas significant at $p < .01$ are surrounded by black contours. B: Decoding performance for selected time windows of interest representing the early (250-350ms; purple) and late (350-500ms; green) time windows of the N300/N400 complex. Performance time-courses represented here reflect the average of performance time-courses of all classifiers trained in the respective time window, i.e., an average of all rows of the GAT matrix shown in 5A within that time window. Significant above chance (>50%) decoding ($p<0.05$, TFCE) is depicted as horizontal solid lines with vertical dashed lines representing the beginning and the end of the significant periods. Shaded region indicates 95% confidence interval. C: Left: Average performance of N300 and N400 time window classifiers in N300 and N400 time windows. Center: performance of decoders specifically trained on averaged N300 or N400 time window activity when generalized to N300 and N400 time window. Right: performance of decoders trained to predict if a data point comes from N300 or N400 time windows.

The early (i.e., N300) classifier reliably predicted activity throughout the entire window of the N300/N400 complex, albeit not up to the full extent of the epoch. Moreover, the late (i.e., N400) classifier generalized beyond its window of training and was able to predict earlier EEG activity (as well as later activity extending up to 800 ms). Figure 5C (left panel) shows that in the N300 time window, N300 classifiers do not perform better than N400 classifiers. During the N300 time window, decoding performance was higher or equivalent for N400 vs. N300 classifiers, but not to a statistically significant degree (all $p > .05$) and with a confidence interval very narrowly centered around zero: N300=>N300 vs. N400-=>N300 mean decoding scores were -0.03 (-.66 to .72), i.e., a substantial advantage of N300 classifiers (over N400 classifiers) when classifying N300 time window activity can be confidently excluded. That means N400 time window classifiers were not any worse at classifying N300 time window patterns than N300 classifiers were. For comparison, the N400 time window is also shown

390 (Figure 5C, left panel). The N400=>N400 result was in fact greater than the N300=>N400
391 decoding (mean: 1.4; 95% CI: .67, 2.21).

392 Finally, we found that classifiers trying to predict if a data slice stemmed from the N300
393 or the N400 time window were at chance performance (both $p > .2$; see Fig. 5C, right).
394 Furthermore, we could not observe any 'home advantage' of N300-trained classifiers when
395 classifying trials based on average activity in that window, compared to N400-trained
396 classifiers, although there was a slight advantage of N400 over N300 classifiers when
397 predicting N400 time window activity (Fig. 5C, center).

4. Discussion

Disentangling the role of contextual scene information in object identification is crucial to understanding the efficiency of perceptual processes. There are different ways in which scene and object processing could interact: scene and object information might be processed in parallel and integrated only post-perceptually (Hollingworth & Henderson, 1999). Or scene information might facilitate the processing of objects already at a perceptual stage, with contextual information reducing the subset of possible object interpretations by activating candidate object representations (Bar, 2004; Brandman & Peelen, 2017; Trapp & Bar, 2015). An established method for investigating the role of scene context on object identification is to violate predicted object-scene pairings. Violations in expected object-scene relationships are associated with two negative ERP deflections: a later (350-500ms) component similar to the N400 in language paradigms (Ganis & Kutas, 2003; Kutas & Federmeier, 2011) and an earlier (250-350 ms) component – referred to as N300 and hypothesized to reflect pre-semantic perceptual processes (Hamm et al., 2002; McPherson & Holcomb, 1999). The N300 has been taken as evidence for contextual information already biasing perceptual processes (Mudrik et al., 2010, 2014; Võ & Wolfe, 2013). This early interaction has been corroborated by high-resolution neuroimaging (Brandman & Peelen, 2017). It remained unresolved, however, if the N300 and N400 components reflect two distinct semantic processes in object identification – categorization and amodal semantic integration respectively – or if they share underlying networks of cortical activity.

In this study, we first of all replicate previous findings of congruency differences in both the N300 and N400 time windows (Mudrik et al., 2010, 2014; Võ & Wolfe, 2013). Beyond that, by applying MVPA to our EEG data, we found shared neural patterns across the observed N300 and N400 components - and therefore no evidence for distinct processes between the early and late object-scene integration stages. This supports the notion that

similar neural patterns are active during both time windows. It argues against the interpretation of these components as reflecting separate perceptual vs. semantic processes. It also suggests the term N300 should be used with caution, or employed purely descriptively, when referring to the early part of the N400, so as to not suggest neurocognitive evidence for two distinct processing stages during this time window.

More generally, our results speak against an interpretation of the ERP as a fixed sequence of time windows, perhaps motivated by directly reading off peaks in the raw waveforms. Many ERP components vary systematically in their latency depending on various experimental or internal contingencies (e.g., Sassenhagen, Schlesewsky, & Bornkessel-Schlesewsky, 2014; Verleger, 1997). Here, we show that essentially the same neurocognitive pattern can extend across what in other research has been understood as boundaries between such windows. That is, semantically inconsistent scene contexts trigger processes that encompass both early and later phases of object processing. In that vein, a recent study by Truman and Mudrik (2018) manipulated both object identifiability and semantic congruence of objects displayed in scenes to test the influence of context on object identification. This study demonstrates that experimental manipulations can distinguish between two functionally different events occurring in the same N300 time window – e.g., object identification based on visual features and semantic incongruence processing. Importantly, the waveforms for semantically incongruent objects diverged from visually unidentifiable ones later than semantically congruent objects, indicating these were only identified as objects later in time; this was taken as evidence for scene contexts affecting object identification. However, these different processes were also reflected in very distinct topographies (with a fronto-central pattern – likely the same pattern we are associating with the N400 here – for inconsistency, and an occipital pattern for object identifiability), indicating that two very different neurocognitive events play out in this time window.

While we do not find evidence for two separate neurocognitive processes underlying both early and later effects of scene contexts on object processing, our findings should also not be overinterpreted. First, while they indicate that some neural sources are activated throughout the combined N300/N400 window, it is also possible that there are other, i.e., distinct neural sources active in the N300 and/or N400 windows which can, however, not be detected with the methods applied here – e.g., non-phase-locked effects, or those with source configurations unlikely to be detected via EEG. Second, in our study the scene and object were sequentially presented. There is evidence from studies providing simultaneous presentation of object and scene (Mudrik et al., 2010, 2014), which indicate a possibly more pronounced N300 response – it might be that such a paradigm is more sensitive to an independent early process. Moreover, while our results indicate that the same neural substrates are active throughout both time windows, this cannot automatically be taken as evidence that only one cognitive process unfolds; rather, the same substrate might in principle be involved in two entirely different processes from one time-point to the next.

As a specific example for how our results do not prove the complete identity between N300 and N400 time window activity, consider that N400 classifiers also perform above chance at later time points than N300 classifiers do. That is, later GAT decoding – in the top right of the GAT matrix – indicate that while N300 activity can be decoded by N400 classifiers as well as by N300 classifiers, N400 classifiers detect their patterns throughout a slightly longer window. In this late window, N300 classifiers no longer pick up activity. Moreover, there was a N400 classifier "home advantage" (see Fig. 6b, right), indicating that N300 time window patterns are a subset of the patterns found in the N400 time window. This could indicate that a further process – e.g., the late positive complex (e.g., Schendan & Kutas, 2002) – begins already towards the edge of the N400 time window, and is partially learned by N400, but not N300 classifiers. That is, both N400 and N300 classifiers are able to learn the pattern occurring in the N400 time window – which is observed throughout both the N300

and N400 time windows; but the N400 classifier additionally picks up on later patterns, perhaps reflecting an already initiated higher-level categorical process (see also Heikel, Sassenhagen & Fiebach, 2018). Evidence for the emergence of such a late positivity can be seen in the topographical maps of Figure 3 and the spatial decoding patterns of Figure 4. This finding, combined with the main finding of the similarity between N300 and N400, also establishes the potential of time-generalized decoding for illustrating the neurocognitive architecture of scene processing. It complements previous methods, and allows a new range of research questions to be addressed.

In sum, our results suggest that scene context already plays a role in early phases of object processing (Bar, 2004; Brandman & Peelen, 2017; Truman & Mudrik, 2018), without necessitating a two-component explanation of such effects. A more precise measurement of the onset of generalization depends on more specialized analyses of time-generalized cross-decoding, operating on higher-powered samples. However, *if* the observation of only one pattern sustained throughout the N300 and N400 time windows indeed indicates just one underlying neural event, then the neural substrates underlying comparatively high-level stages in scene processing/object-scene integration are already active very early, perhaps as early as 200 msec post stimulus presentation.

References

Bar, M. (2004). Visual objects in context. *Nature Reviews Neuroscience*, *5*(8), 617–629. https://doi.org/10.1038/nrn1476

Bar, M. (2007). The proactive brain: using analogies and associations to generate predictions. *Trends in Cognitive Sciences*, *11*(7), 280–289. https://doi.org/10.1016/j.tics.2007.05.005

Bar, M. (2009). The proactive brain: memory for predictions. *Philosophical Transactions of the Royal Society of London. Series B, Biological Sciences*, *364*(1521), 1235–1243. https://doi.org/10.1098/rstb.2008.0310

Biederman. (1981). On the semantics of a glance at a scene. In M. Kubovy & J. R. Pomerantz (Eds.), *Perceptual Organization* (pp. 213–263). Hillsdale, New Jersey: Lawrence Erlbaum. Retrieved from http://www.citeulike.org/user/ChristinaPavlo/article/6541577

Biederman, I., Mezzanotte, R. J., & Rabinowitz, J. C. (1982). Scene perception: detecting and judging objects undergoing relational violations. *Cognitive Psychology*, *14*(2), 143–177.

Brandman, T., & Peelen, M. V. (2017). Interaction between Scene and Object Processing Revealed by Human fMRI and MEG Decoding. *Journal of Neuroscience*, *37*(32). Retrieved from http://www.jneurosci.org/content/37/32/7700

Castelhano, M. S., & Heaven, C. (2011). Scene context influences without scene gist: eye movements guided by spatial associations in visual search. *Psychonomic Bulletin & Review*, *18*(5), 890–896. article. https://doi.org/10.3758/s13423-011-0107-8

Cornelissen, T. H. W., & Võ, M. L.-H. (2016). Stuck on semantics: Processing of irrelevant object-scene inconsistencies modulates ongoing gaze behavior. *Attention, Perception & Psychophysics*. https://doi.org/10.3758/s13414-016-1203-7

Davenport, J. L., & Potter, M. C. (2004). Scene consistency in object and background perception. *Psychological Science*, *15*(8), 559–564. https://doi.org/10.1111/j.0956-7976.2004.00719.x

Demiral, Ş. B., Malcolm, G. L., & Henderson, J. M. (2012). ERP correlates of spatially incongruent object identification during scene viewing: Contextual expectancy versus simultaneous processing. *Neuropsychologia*, *50*, 1271–1285.

Draschkow, D., & Võ, M. L.-H. (2017). Scene grammar shapes the way we interact with objects, strengthens memories, and speeds search. *Scientific Reports*, *7*(1), 16471. https://doi.org/10.1038/s41598-017-16739-x

Federmeier, K. D., & Kutas, M. (2001). Meaning and modality: Influences of context, semantic memory organization, and perceptual predictability on picture processing. *Journal of Experimental Psychology: Learning, Memory, and Cognition*, *27*(1), 202–224. https://doi.org/10.1037/0278-7393.27.1.202

Ganis, G., & Kutas, M. (2003). An electrophysiological study of scene effects on object identification. *Cognitive Brain Research*, *16*(2), 123–144. https://doi.org/10.1016/S0926-6410(02)00244-6

Ganis, G., Kutas, M., & Sereno, M. I. (1996). The Search for "Common Sense": An Electrophysiological Study of the Comprehension of Words and Pictures in Reading. *Journal of Cognitive Neuroscience*, *8*(2), 89–106. https://doi.org/10.1162/jocn.1996.8.2.89

Gramfort, A., Luessi, M., Larson, E., Engemann, D. A., Strohmeier, D., Brodbeck, C., … Hämäläinen, M. (2013). MEG and EEG data analysis with MNE-Python. *Frontiers in Neuroscience*, *7*, 267. https://doi.org/10.3389/fnins.2013.00267

Hamm, J. P., Johnson, B. W., & Kirk, I. J. (2002). Comparison of the N300 and N400 ERPs to picture stimuli in congruent and incongruent contexts. *Clinical Neurophysiology : Official Journal of the International Federation of Clinical Neurophysiology*, *113*(8), 1339–1350. Retrieved from http://www.ncbi.nlm.nih.gov/pubmed/12140015

Haufe, S., Meinecke, F., Görgen, K., Dähne, S., Haynes, J.-D., Blankertz, B., & Bießmann, F. (2014). On the interpretation of weight vectors of linear models in multivariate neuroimaging. *NeuroImage*, *87*, 96–110. https://doi.org/10.1016/J.NEUROIMAGE.2013.10.067

Heikel, E., Sassenhagen, J., & Fiebach, C. J. (2018). Time-generalized multivariate analysis of EEG responses reveals a cascading architecture of semantic mismatch processing. *Brain and Language*, *184*, 43–53. https://doi.org/10.1016/J.BANDL.2018.06.007

Henderson, J. M., Weeks, P. A., & Hollingworth, A. (1999). The effects of semantic consistency on eye movements during complex scene viewing. *Journal of Experimental Psychology. Human Perception and Performance*, *25*(1), 210–228. Retrieved from http://psycnet.apa.orgjournals/xhp/25/1/210

Hollingworth, A., & Henderson, J. M. (1999). Object identification is isolated from scene semantic constraint: evidence from object type and token discrimination. *Acta Psychologica*, *102*(2–3), 319–343. https://doi.org/10.1016/S0001-6918(98)00053-5

Jas, M., Engemann, D. A., Bekhti, Y., Raimondo, F., & Gramfort, A. (2017). Autoreject: Automated artifact rejection for MEG and EEG data. *NeuroImage*, *159*, 417–429. https://doi.org/10.1016/J.NEUROIMAGE.2017.06.030

Jung, T.-P., Makeig, S., Humphries, C., Lee, T.-W., McKeown, M. J., Iragui, V., & Sejnowski, T. J. (2000). Removing electroencephalographic artifacts by blind source separation. *Psychophysiology*, *37*(2), 163–178. https://doi.org/10.1111/1469-8986.3720163

King, J.-R., & Dehaene, S. (2014). Characterizing the dynamics of mental representations: the temporal generalization method. *Trends in Cognitive Sciences*, *18*(4), 203–210. https://doi.org/10.1016/j.tics.2014.01.002

Kluyver, T., Ragan-Kelley, B., Pérez, F., Granger, B., Bussonnier, M., Frederic, J., … Willing, C. (2016). Jupyter Notebooks -- a publishing format for reproducible computational workflows. In F. Loizides & B. Schmidt (Eds.), *Positioning and Power in Academic Publishing: Players, Agents and Agendas* (pp. 87–90).

Kovalenko, L. Y., Chaumon, M., & Busch, N. A. (2012). A pool of pairs of related objects (POPORO) for investigating visual semantic integration: behavioral and electrophysiological validation. *Brain Topography*, *25*(3), 272–284. https://doi.org/10.1007/s10548-011-0216-8

Kutas, M., & Federmeier, K. D. (2011). Thirty years and counting: finding meaning in the N400 component of the event-related brain potential (ERP). *Annual Review of Psychology*, *62*, 621–647. https://doi.org/10.1146/annurev.psych.093008.131123

Kutas, M., & Hillyard, S. A. (1980). Reading Senseless Sentences: Brain Potentials Reflect Semantic Incongruity. *Science*, *207*, 203–205.

Loftus, G. R., & Mackworth, N. H. (1978). Cognitive determinants of fixation location during picture viewing. *Journal of Experimental Psychology. Human Perception and Performance*, *4*(4), 565–572.

Maris, E., & Oostenveld, R. (2007). Nonparametric statistical testing of EEG- and MEG-data. *Journal of Neuroscience Methods*, *164*(1), 177–190. https://doi.org/10.1016/J.JNEUMETH.2007.03.024

Mathôt, S., Schreij, D., & Theeuwes, J. (2012). OpenSesame: An open-source, graphical experiment builder for the social sciences. *Behavior Research Methods*, *44*(2), 314–324. https://doi.org/10.3758/s13428-011-0168-7

McPherson, B. W., & Holcomb, P. J. (1999). An electrophysiological investigation of semantic priming with pictures of real objects. *Psychophysiology*, *36*(1), 53–65. Retrieved from http://www.ncbi.nlm.nih.gov/pubmed/10098380

Meade, G., Lee, B., Midgley, K. J., Holcomb, P. J., & Emmorey, K. (2018). Phonological and semantic priming in American Sign Language: N300 and N400 effects. *Language, Cognition and Neuroscience*, 1–15. https://doi.org/10.1080/23273798.2018.1446543

Mudrik, L., Lamy, D., & Deouell, L. Y. (2010). ERP evidence for context congruity effects during simultaneous object-scene processing. *Neuropsychologia*, *48*(2), 507–517. https://doi.org/10.1016/j.neuropsychologia.2009.10.011

Mudrik, L., Shalgi, S., Lamy, D., & Deouell, L. Y. (2014). Synchronous contextual irregularities affect early scene processing: Replication and extension. *Neuropsychologia*, *56*(1), 447–458. https://doi.org/10.1016/j.neuropsychologia.2014.02.020

Nigam, A., Hoffman, J. E., & Simons, R. F. (1992). N400 to Semantically Anomalous Pictures and Words. *Journal of Cognitive Neuroscience*, *4*(1), 15–22. https://doi.org/10.1162/jocn.1992.4.1.15

Nobre, A. C., & McCarthy, G. (1994). Language-Related ERPs: Scalp Distributions and Modulation by Word Type and Semantic Priming. *Journal of Cognitive Neuroscience*, *6*(3), 233–255. https://doi.org/10.1162/jocn.1994.6.3.233

Pedregosa, F., Varoquaux, G., Gramfort, A., Michel, V., Thirion, B., Grisel, O., … Duchesnay, É. (2011). Scikit-learn: Machine Learning in Python. *Journal of Machine Learning Research*, *12*(Oct), 2825–2830. Retrieved from http://www.jmlr.org/papers/v12/pedregosa11a.html

Sassenhagen, J., Schlesewsky, M., & Bornkessel-Schlesewsky, I. (2014). The P600-as-P3 hypothesis revisited: Single-trial analyses reveal that the late EEG positivity following linguistically deviant material is reaction time aligned. *Brain and Language*, *137*, 29–39. https://doi.org/10.1016/J.BANDL.2014.07.010

Schendan, H., & Kutas, M. (2002). Neurophysiological evidence for two processing times for visual object identification. *Neuropsychologia*, *40*(7), 931–945. https://doi.org/10.1016/S0028-3932(01)00176-2

Schendan, H., & Maher, S. (2009). Object knowledge during entry-level categorization is activated and modified by implicit memory after 200 ms. *NeuroImage*, *44*(4), 1423–1438. https://doi.org/10.1016/j.neuroimage.2008.09.061

Sitnikova, T., Holcomb, P. J., Kiyonaga, K. A., & Kuperberg, G. R. (2008). Two neurocognitive mechanisms of semantic integration during the comprehension of visual real-world events. *Journal of Cognitive Neuroscience*, *20*(11), 2037–2057. https://doi.org/10.1162/jocn.2008.20143

Smith, S. M., & Nichols, T. E. (2009). Threshold-free cluster enhancement: Addressing problems of smoothing, threshold dependence and localisation in cluster inference. *NeuroImage*, *44*(1), 83–98. https://doi.org/10.1016/J.NEUROIMAGE.2008.03.061

Trapp, S., & Bar, M. (2015). Prediction, context, and competition in visual recognition. *Annals of the New York Academy of Sciences*, *1339*(1), 190–198. https://doi.org/10.1111/nyas.12680

Truman, A., & Mudrik, L. (2018). Are incongruent objects harder to identify? The functional significance of the N300 component. *Neuropsychologia*, *117*, 222–232. https://doi.org/10.1016/j.neuropsychologia.2018.06.004

Urbach, T. P., & Kutas, M. (2002). The intractability of scaling scalp distributions to infer neuroelectric sources. *Psychophysiology*, *39*(6), 791–808. https://doi.org/10.1017/S0048577202010648

Verleger, R. (1997). On the utility of P3 latency as an index of mental chronometry. *Psychophysiology*, *34*(2), 131–156. https://doi.org/10.1111/j.1469-8986.1997.tb02125.x

Viola, F. C., Thorne, J., Edmonds, B., Schneider, T., Eichele, T., & Debener, S. (2009). Semi-automatic identification of independent components representing EEG artifact. *Clinical Neurophysiology*, *120*(5), 868–877. https://doi.org/10.1016/J.CLINPH.2009.01.015

Võ, M. L.-H., & Henderson, J. M. (2010). The time course of initial scene processing for eye movement guidance in natural scene search. *Journal of Vision*, *10*(3), 14.1-13. https://doi.org/10.1167/10.3.14

Võ, M. L.-H., & Wolfe, J. M. (2013). Differential electrophysiological signatures of semantic and syntactic scene processing. *Psychological Science*, *24*(9), 1816–1823.

https://doi.org/10.1177/0956797613476955

Võ, M. L.-H., & Wolfe, J. M. (2015). The role of memory for visual search in scenes. *Annals of the New York Academy of Sciences*, *1339*, 72–81. https://doi.org/10.1111/nyas.12667

Willems, R. M., Özyürek, A., & Hagoort, P. (2008). Seeing and Hearing Meaning: ERP and fMRI Evidence of Word versus Picture Integration into a Sentence Context. *Journal of Cognitive Neuroscience*, *20*(7), 1235–1249. https://doi.org/10.1162/jocn.2008.20085